JAIST Repository
https://dspace.jaist.ac.jp/

Title	Formation of Ohmic Carrier Injection at Anode/organic Interfaces and Carrier Transport Mechanisms of Organic Thin Films
Author(s)	Matsushima, Toshinori; Jin, Guang-He; Kanai, Yoshihiro; Yokota, Tomoyuki; Kitada, Seiki; Kishi, Toshiyuki; Murata, Hideyuki
Citation	Materials Research Society Symposium Proceedings, 1154: 1154-B10-92
Issue Date	2009
Type	Conference Paper
Text version	publisher
URL	http://hdl.handle.net/10119/9843
Rights	Copyright (C) 2009 Materials Research Society. It is posted here by permission of the Materials Research Society. Toshinori Matsushima, Guang-He Jin, Yoshihiro Kanai, Tomoyuki Yokota, Seiki Kitada, Toshiyuki Kishi, and Hideyuki Murata, Materials Research Society Symposium Proceedings, 1154, 2009, 1154-B10-92. http://www.mrs.org/
Description	

JAIST
JAPAN
ADVANCED INSTITUTE OF
SCIENCE AND TECHNOLOGY

Japan Advanced Institute of Science and Technology

Mater. Res. Soc. Symp. Proc. Vol. 1154 © 2009 Materials Research Society 1154-B10-92

Formation of Ohmic Carrier Injection at Anode/Organic Interfaces and Carrier Transport Mechanisms of Organic Thin Films

Toshinori Matsushima, Guang-He Jin, Yoshihiro Kanai, Tomoyuki Yokota, Seiki Kitada, Toshiyuki Kishi, and Hideyuki Murata *

School of Materials Science, Japan Advanced Institute of Science and Technology, 1-1 Asahidai, Nomi, Ishikawa 923-1292, Japan

*Corresponding author. Tel.: +81 761 51 1531; fax: +81 761 51 1149;
E-mail address: murata-h@jaist.ac.jp

ABSTRACT

We have shown that hole mobilities of a wide variety of organic thin films can be estimated using a steady-state space-charge-limited current (SCLC) technique due to formation of Ohmic hole injection by introducing a very thin hole-injection layer of molybdenum oxide (MoO_3) between an indium tin oxide anode layer and an organic hole-transport layer. Organic hole-transport materials used to estimate hole mobilities are 4,4',4"-tris(*N*-3-methylphenyl-*N*-phenyl-amino)triphenylamine (m-MTDATA), 4,4',4"-tris(*N*-2-naphthyl-*N*-phenyl-amino)triphenylamine (2-TNATA), rubrene, *N*,*N*´-di(m-tolyl)-*N*,*N*´-diphenylbenzidine (TPD), and *N*,*N*´-diphenyl-*N*,*N*´-bis(1-naphthyl)-1,1´-biphenyl-4,4´-diamine (α-NPD). These materials are found to have electric-field-dependent hole mobilities. While field dependence parameters (β) estimated from SCLCs are almost similar to those estimated using a widely used time-of-flight (TOF) technique, zero field SCLC mobilities (μ_0) are about one order of magnitude lower than zero field TOF mobilities.

INTRODUCTION

Organic light-emitting diodes (OLEDs) have been developed due to their high potentials for use in low-cost, mechanically flexible, light-weight display and lighting applications. Multilayer OLEDs are typically composed of an indium tin oxide (ITO) anode, an organic hole-transport layer (HTL), an emitting layer, an electron-transport layer, and a metal cathode. In general, a large hole injection barrier height of several hundred meV is present between an ITO layer and an HTL, which causes an increase in driving voltage of OLEDs. Various organic and inorganic hole-injection layers (HILs) have been inserted between an ITO and an HTL to reduce the driving voltages [1-3]. Recently, we have demonstrated that the use of a 0.75 nm HIL of molybdenum oxide (MoO_3) inserted between an ITO and an HTL of *N*,*N*´-diphenyl-*N*,*N*´-bis(1-naphthyl)-1,1´-biphenyl-4,4´-diamine (α-NPD) leads to the formation of an Ohmic contact at the ITO/MoO_3/α-NPD interfaces and the observation of a space-charge-limited current (SCLC) of α-NPD [4]. This MoO_3 thickness of 0.75 nm is much thinner than the previously reported values. Moreover, marked improvements of driving voltages, power conversion efficiencies, and operational stability of OLEDs have been realized using the very thin MoO_3 HIL [5,6].

Presence of charge-carrier injection barriers at electrode/organic interfaces generally makes it difficult to investigate carrier transport mechanisms in organic films because observed currents are governed by both carrier injection and transport [7]. In this study, we have shown that Ohmic contacts can be formed and SCLCs can be observed using a very thin MoO_3 HIL between an ITO anode layer and a wide variety of organic HTLs. Organic HTL materials used in this study are 4,4',4"-tris(*N*-3-methylphenyl-*N*-phenyl-amino)triphenylamine (m-MTDATA), 4,4',4"-tris(*N*-2-naphthyl-*N*-phenyl-amino)triphenylamine (2-TNATA), rubrene, *N*,*N*´-di(m-tolyl)-*N*,*N*´-diphenylbenzidine (TPD), α-NPD, 5,10,15,20-tetraphenylporphyrin (H_2TPP), and 2,4,6-tricarbazolo-1,3,5-triazine (TRZ-2). The chemical structures of the organic HTL molecules are shown in figure 1. From analyses of current density-voltage (*J*-*V*) characteristics of the HTLs with a SCLC equation, we found that while field dependence parameters (β) estimated from SCLC regions are almost similar to those estimated using a widely used time-of-flight (TOF) technique, zero field SCLC mobilities (μ_0) are about one order of magnitude lower than zero field TOF mobilities.

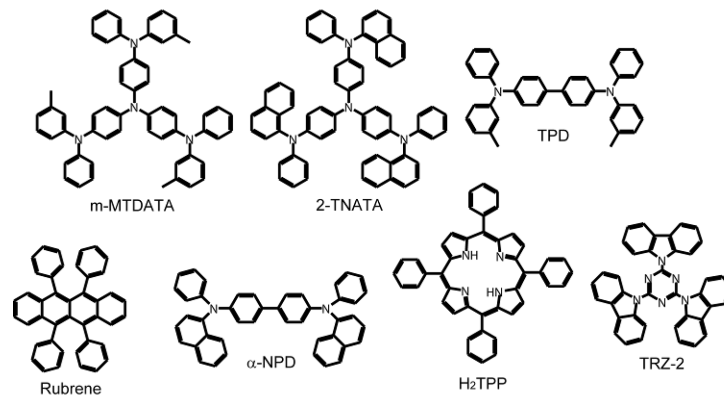

Figure 1. Chemical structures of organic molecules used to estimate hole mobilities.

EXPERIMENT

The schematic structure of the single-organic-layer, hole-carrier-only devices used in this study are shown in figure 2(a). The hole-only devices consisted of a glass substrate coated with a 150 nm ITO anode layer, a *X* nm MoO_3 HIL, a 100 nm organic HTL, an electron-blocking layer (EBL) of MoO_3, and a 100 nm cathode layer of Al. The devices were fabricated using a preparation condition as previously reported in Refs. [4-6]. The organic materials shown in figure 1 were used as the HTLs. The thicknesses of the MoO_3 HIL (*X*) between the ITO and the HTL were varied from 0 nm to 10 nm. The completed devices were encapsulated using a glass cap and an ultraviolet curing epoxy resin inside a nitrogen-filled glove box. The steady-state *J*-*V* characteristics of the devices with various *X* were measured using a SCS4200 semiconductor characterization system (Keithley) under dark at room temperature.

50 nm layers of the organic and inorganic materials were prepared on cleaned ITO surfaces to determine their ionization potential and work function energy levels by using an AC-2 photoelectron yield spectrometer (Riken Keiki). The electron affinity energy levels of the

organic layers were roughly estimated by subtracting their optical absorption onset energies from the ionization potential energy levels. The energy-level diagram of the devices with the values thus measured is depicted in figure 2(b). The hole injection and transport characteristics of the devices were investigated by changing the ionization potential energy levels of the HTLs from -5.06 eV (m-MTDATA) to -5.13 eV (2-TNATA), -5.24 eV (TPD), -5.29 eV (rubrene), -5.40 eV (α-NPD), -5.52 eV (H_2TPP), and -5.68 eV (TRZ-2) relative to the work function of ITO (-5.02 eV). As shown in figure 2(b), high-work-function MoO_3 (-5.68 eV) was introduced as the EBL between the HTL and the Al cathode to prevent electron injection from the cathode. In fact, all devices exhibited no electroluminescence from the HTLs during the *J-V* measurements, indicating that unipolar hole currents flow through the devices.

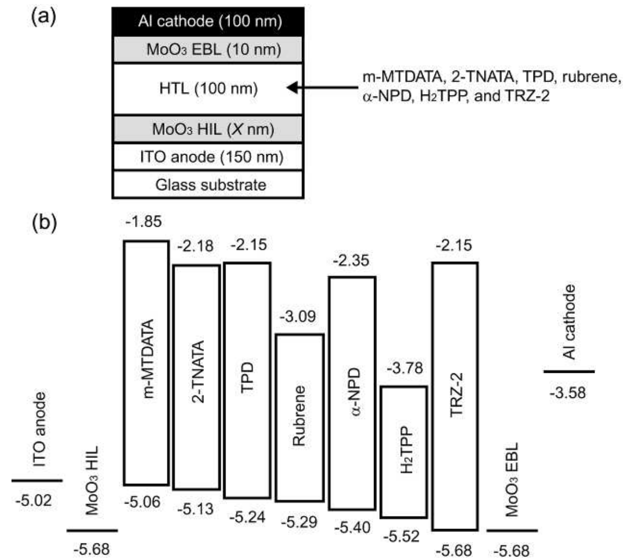

Figure 2. (a) Schematic structure of hole-only devices and (b) energy-level diagram of hole-only devices. Thicknesses of MoO_3 HIL used between ITO and HTL were varied from 0 nm to 10 nm.

RESULTS AND DISCUSSION

If an Ohmic contact is formed and a free charge density is negligible in comparison to an injected charge density, a SCLC with field-dependent carrier mobilities [8,9] is given by

$$J = \frac{9}{8}\varepsilon_r \varepsilon_0 \mu_0 \exp(0.89\beta\left(\frac{V}{L}\right)^{0.5})\frac{V^2}{L^3} \quad (1),$$

where ε_r is the relative permittivity, ε_0 is the vacuum permittivity, μ_0 is the zero field mobility, β is the field dependence parameter, and L is the cathode-anode spacing. By fitting the *J-V* characteristics of the hole-only devices with Eq. (1), μ_0 and β values of the HTLs can be estimated at the same time. In this study, a standard ε_r of 3.0 for organic thin films was used to fitting.

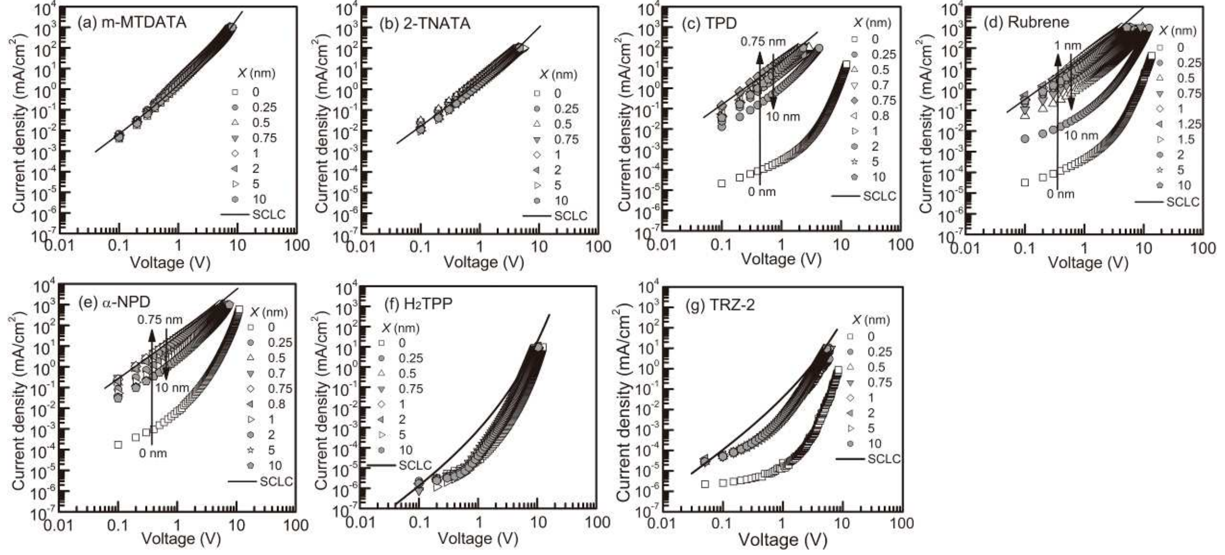

Figure 3. *J*-*V* characteristics of hole-only devices with HTLs of (a) m-MTDATA, (b) 2-TNATA, (c) TPD, (d) rubrene, (e) α-NPD, (f) H_2TPP, and (g) TRZ-2. The solid curves represent calculated *J*-*V* curves based on Eq. (1).

The *J*-*V* characteristics of m-MTDATA and 2-TNATA are independent of the oxide thicknesses *X* and are well fitted with Eq. (1) [the solid curves in figures 3(a) and 3(b)]. The μ_0 and β estimated by the fitting are (1.5 ± 0.1) x 10^{-6} cm^2 V^{-1} s^{-1} and (3.7 ± 0.4) x 10^{-3} $cm^{0.5}$ $V^{-0.5}$ for m-MTDATA and (4.5 ± 0.3) x 10^{-6} cm^2 V^{-1} s^{-1} and (2.0 ± 0.2) x 10^{-3} $cm^{0.5}$ $V^{-0.5}$ for 2-TNATA, respectively. These results indicate that the *J*-*V* characteristics are controlled by the SCLCs and the ITO/m-MTDATA and ITO/2-TNATA junctions are already Ohmic contacts without the MoO_3 HILs. The hole injection barrier heights are estimated from figure 2(b) to be 0.04 eV at the ITO/m-MTDATA interface and 0.11 eV at the ITO/2-TNATA interface. We assume that the very small barrier heights less than ≈ 0.1 eV no longer prevent hole injection from the ITO. It has been reported that ITO forms ideal hole-injecting contacts with m-MTDATA [10] and 2-TNATA [11], which is in good agreement with the present results.

The *J*-*V* characteristics of TPD, rubrene, and α-NPD are markedly dependent upon the *X*. The *J*-*V* characteristics of these HTLs shift to higher current densities and then shift to lower current densities as increasing the *X* from 0 nm to 10 nm [figures 3(c), 3(d), and 3(e)]. The similar change in *J*-*V* characteristics has been observed [4]. The optimized *X* is 1.0 nm for rubrene and 0.75 nm for TPD and α-NPD, which provide the highest current densities for the devices. The *J*-*V* characteristics at the optimized *X* are well fitted with Eq. (1) [the solid curves in figures 3(c), 3(d), and 3(e)], yielding a μ_0 of (4.5 ± 0.4) x 10^{-5} cm^2 V^{-1} s^{-1} and a β of (1.5 ± 0.2) x 10^{-3} $cm^{0.5}$ $V^{-0.5}$ for TPD, a μ_0 of (1.0 ± 0.1) x 10^{-4} cm^2 V^{-1} s^{-1} and a β of (1.1 ± 0.2) x 10^{-3} $cm^{0.5}$ $V^{-0.5}$ for rubrene, and a μ_0 of (8.1 ± 0.6) x 10^{-5} cm^2 V^{-1} s^{-1} and a β of (8.0 ± 0.6) x 10^{-4} $cm^{0.5}$ $V^{-0.5}$ for α-NPD.

As can been seen in figure 2(b), the relatively large hole injection barriers are present between the ITO and the HTLs of TPD, rubrene, and α-NPD. However, these barrier heights are lowered by using the very thin MoO_3 HIL to form Ohmic hole injection due probably to an increase in work function of an ITO/MoO_3 anode [6] and efficient hole injection via gap states caused by an electron transfer from the HTLs to the MoO_3 HIL [12]. On the other hands, we

suppose that a strong space charge layer is formed in the HTLs due to the electron transfer when the thick MoO_3 HIL is used. The strong space charge layer may lower carrier injection at the interfaces, resulting in a decrease in current density at higher *X*, as shown in figures 3(c), 3(d), and 3(e).

The *J*-*V* characteristics of the hole-only devices with the H_2TPP HTL and the TRZ-2 HTL are shown in figures 3(f) and 3(g). The *J*-*V* characteristics are not well explained with Eq. (1) [the solid lines in figures 3(f) and 3(g)], indicating that the *J*-*V* characteristics are controlled by injection-limited currents. Since the ionization potential energies of H_2TPP and TRZ-2 are deeper than those of the other HTL materials (figure 2), Ohmic conductions are not realized even by using the MoO_3 HIL.

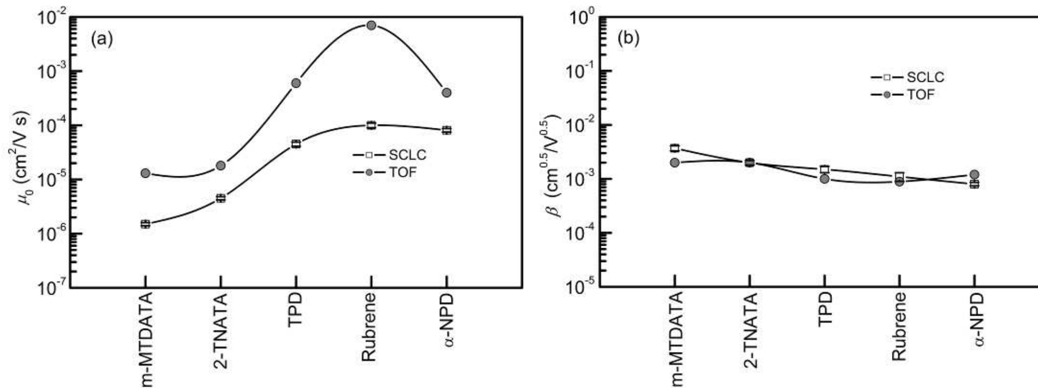

Figure 4. Comparison of μ_0 and β estimated from SCLC and TOF techniques.

The μ_0 and β estimated from the SCLC regions are compared with those of m-MTDATA [13], 2-TNATA [11], TPD [14], rubrene [15], and α-NPD [14] previously estimated using a TOF technique. The comparison results of the μ_0 and the β are shown in figures. 4(a) and 4(b), respectively. While the β estimated from the SCLCs is almost similar to that estimated using a TOF technique, the μ_0 estimated from the SCLCs is about one order of magnitude lower than that estimated using a TOF technique. It has been shown that electron mobilities of tris(8-hydroxyquinoline) aluminum (Alq_3) [16] and 4,7-diphenyl-1,10-phenanthroline (Bphen) [17] and hole mobilities of α-NPD [18] and m-MTDATA [19] gradually decrease with decreasing their film thicknesses. Chu *et al.* attributed the thickness-dependent mobilities to a change of hole trap concentrations in films [18]. Thus, we infer that SCLC mobilities measured from thinner films become lower than TOF mobilities measured from thicker films.

CONCLUSIONS

In this study, we investigated that how thicknesses of a MoO_3 HIL inserted between an ITO layer and a wide variety of organic HTLs influence *J*-*V* characteristics of hole-only devices. We obtained the following relationships between hole injection barrier heights and *J*-*V* characteristics. (1) Small barrier heights less than ≈ 0.1 eV at interfaces of ITO/m-MTDATA and ITO/2-TNATA no longer prevent hole injection from the ITO (Ohmic contacts). Thus, SCLCs of m-MTDATA and 2-TNATA are observed without a MoO_3 HIL. (2) Barrier heights ranging from ≈ 0.1 eV to ≈ 0.5 eV at interfaces of ITO/TPD, ITO/rubrene, and ITO/α-NPD lower hole

injection. However, introduction of a very thin MoO_3 HIL at the interfaces leads to formation of Ohmic contacts and observation of their SCLCs. (3) Barrier heights larger than ≈ 0.5 eV at interfaces of ITO/H_2TPP and ITO/TRZ-2 markedly lower hole injection. Ohmic contacts are not realized at the interfaces even by using a MoO_3 HIL. Moreover, by analyzing *J-V* characteristics of the organic HTLs with a SCLC equation, we obtained μ_0 and β, as summarized in table I. The μ_0 estimated from the SCLC regions is found to be lower than those estimated using a TOF technique. We believe that these findings are indispensable to clarifying carrier injection and transport mechanisms of organic thin films and to developing OLEDs.

Table I. μ_0 and β estimated from SCLCs

HTL material	μ_0 ($cm^2\ V^{-2}\ s^{-1}$)	β ($cm^{0.5}\ V^{-0.5}$)
m-MTDATA	$(1.5 \pm 0.1) \times 10^{-6}$	$(3.7 \pm 0.4) \times 10^{-3}$
2-TNATA	$(4.5 \pm 0.3) \times 10^{-6}$	$(2.0 \pm 0.2) \times 10^{-3}$
TPD	$(4.5 \pm 0.4) \times 10^{-5}$	$(1.5 \pm 0.2) \times 10^{-3}$
Rubrene	$(1.0 \pm 0.1) \times 10^{-4}$	$(1.1 \pm 0.2) \times 10^{-3}$
α-NPD	$(8.1 \pm 0.6) \times 10^{-5}$	$(8.0 \pm 0.6) \times 10^{-4}$

REFERENCES

(1) S. A. VanSlyke, C. H. Chen, and C. W. Tang, *Appl. Phys. Lett.* **69**, 2160 (1996).
(2) S.-F. Chen and C.-W. Wang, *Appl. Phys. Lett.* **85**, 765 (2004).
(3) S. Tokito, K. Noda, and Y. Taga, *J. Phys. D: Appl. Phys.* **29**, 2750 (1996).
(4) T. Matsushima, Y. Kinoshita, and H. Murata, *Appl. Phys. Lett.* **91**, 253504 (2007).
(5) T. Matsushima and H. Murata, *J. Appl. Phys.* **104**, 034507 (2008).
(6) T. Matsushima, G.-H. Jin, and H. Murata, *J. Appl. Phys.* **104**, 054501 (2008).
(7) M. Abkowitz, J. S. Facci, and J. Rehm, *J. Appl. Phys.* **83**, 2670 (1998).
(8) M. A. Lampert and P. Mark, *Current Injection In Solids* (ACADEMIC, New York, 1970).
(9) P. N. Murgatroyd*, J. Phys. D: Appl. Phys.* **3**, 151 (1970)
(10) C. Giebeler, H. Antoniadis, D. D. C. Bradley, and Y. Shirota, *Appl. Phys. Lett.* **72**, 2448 (1998).
(11) C. H. Cheung, K. C. Kwok, S. C. Tse, and S. K. So, *J. Appl. Phys.* **103**, 093705 (2008).
(12) H. Lee, S. W. Cho, K. Han, P. E. Jeon, C.-N. Whang, K. Jeong, K. Cho, and Y. Yi, *Appl. Phys. Lett.* **93**, 043308 (2008).
(13) S. W. Tsang, S. K. So, and J. B. Xu, *J. Appl. Phys.* **99**, 013706 (2006).
(14) S. Naka, H. Okada, H. Onnagawa, Y. Yamaguchi, and T. Tsutsui, *Synth. Met.* **111-112**, 331 (2000).
(15) H. H. Fong, S. K. So, W. Y. Sham, C. F. Lo, Y. S. Wu, and C. H. Chen, *Chem. Phys. Lett.* **298**, 119 (2004).
(16) S. C. Tse, H. H. Fong, and S. K. So, *J. Appl. Phys.* **94,** 2033 (2003).
(17) W. Xu, Khizar-ul-Haq, Y. Bai, X. Y. Jiang, and Z. L. Zhang, *Solid State Communications* **146,** 311 (2008).
(18) T. Y. Chu and O. K. Song, *Appl. Phys. Lett.* **90**, 203512 (2007).
(19) O. J. Weiß, R. K. Krause, and A. Hunze, *J. Appl. Phys.* **103,** 043709 (2008).